



A catalog of bright calibrator stars for 200-meter baseline near-infrared stellar interferometry

Mérand Antoine, Pascal Bordé, Vincent Coude Du Foresto

► To cite this version:

Mérand Antoine, Pascal Bordé, Vincent Coude Du Foresto. A catalog of bright calibrator stars for 200-meter baseline near-infrared stellar interferometry. *Astronomy and Astrophysics - A&A*, 2005, 433, pp.1155. hal-00005681

HAL Id: hal-00005681

<https://hal.science/hal-00005681>

Submitted on 28 Jun 2005

HAL is a multi-disciplinary open access archive for the deposit and dissemination of scientific research documents, whether they are published or not. The documents may come from teaching and research institutions in France or abroad, or from public or private research centers.

L'archive ouverte pluridisciplinaire **HAL**, est destinée au dépôt et à la diffusion de documents scientifiques de niveau recherche, publiés ou non, émanant des établissements d'enseignement et de recherche français ou étrangers, des laboratoires publics ou privés.

A catalog of bright calibrator stars for 200-meter baseline near-infrared stellar interferometry[★]

Antoine Mérand¹, Pascal Bordé^{2,★★}, and Vincent Coudé du Foresto¹

¹ LESIA, UMR8109, Observatoire de Paris, 5 place Jules Janssen, 92195 Meudon, France
e-mail: Antoine.Merand@obspm.fr, Vincent.Foresto@obspm.fr

² Harvard-Smithsonian Center for Astrophysics, 60 Garden Street, Cambridge, MA 02138, USA
e-mail: pborde@cfa.harvard.edu

Received — / Accepted —

Abstract. We present in this paper a catalog of reference stars suitable for calibrating infrared interferometric observations. In the K band, visibilities can be calibrated with a precision of 1 % on baselines up to 200 meters for the whole sky, and up to 300 meters for some part of the sky. This work, extending to longer baselines a previous catalog compiled by Bordé et al. (2002), is particularly well adapted to hectometric-class interferometers such as the Very Large Telescope Interferometer (VLTI, Glindemann et al. 2003) or the CHARA array (ten Brummelaar et al. 2003) when one is observing well-resolved, high-surface brightness objects ($K \lesssim 8$). We use the absolute spectro-photometric calibration method introduced by Cohen et al. (1999) to derive the angular diameters of our new set of 948 G8–M0 calibrator stars extracted from the IRAS, 2MASS and MSX catalogs. Angular stellar diameters range from 0.6 mas to 1.8 mas (median is 1.1 mas) with a median precision of 1.35 %. For both the northern and southern hemispheres, the closest calibrator star is always less than 10° away.

Key words. catalogs – stars: fundamental parameters – techniques: interferometric

1. Introduction

Long baseline stellar interferometers measure the amount of coherence (ie the squared modulus of the coherence factor, sometimes also called the raw visibility amplitude, or raw fringe contrast) between any pair of their subapertures. This quantity needs to be calibrated in order to yield the true visibility of the source, which is the modulus of the Fourier transform of the object's intensity distribution at the spatial frequency B/λ defined by the projected baseline B and the wavelength λ . The squared visibility V^2 of an object is derived from the measure μ^2 of its coherence factor, and from an *interferometric efficiency* factor \mathcal{T}^2 (also called *transfer function*), which accounts for the coherence losses caused by imperfections of the instrument and by the Earth's turbulent atmosphere:

$$V^2 = \frac{\mu^2}{\mathcal{T}^2}. \quad (1)$$

From Eq. (1), it appears that the errors in \mathcal{T}^2 and μ^2 contribute equally to the accuracy of the object squared visibility V^2 . As the interferometric efficiency varies during the night

owing to changing instrumental and atmospheric conditions, it has to be frequently sampled, and then interpolated for the time of the science target observation (one can see for example Perrin (1998) for details of an interpolation strategy) to ensure a reliable calibration. The \mathcal{T}^2 determination is done by observing a reference source ($\mu_{\text{cal.}}^2$) with a known squared visibility ($V_{\text{cal.}}^2$), for which

$$\mathcal{T}^2 \equiv \frac{\mu_{\text{cal.}}^2}{V_{\text{cal.}}^2}. \quad (2)$$

In practice, observations of the science target are interleaved with observations of reference stars, referred to as *calibrator stars* or *calibrators* for short. The choice of a calibrator is critical as one should be able to predict its intrinsic visibility at the projected baseline of the interferometer, with an accuracy which should be at least as good as the measurement of the raw visibility (more about this in Sect. 2). For this purpose, Bordé et al. (2002) carefully extracted a catalog of calibrator stars from the spectro-photometric reference stellar network compiled by Cohen et al. (1999), hereafter C99. Because of the estimated angular diameter of the selected stars (typically 2.3 mas with an error of 1.2 %), this catalog, hereafter Cat. 1, provides calibrators for interferometric baselines up to ~ 100 m in the near infrared. The advent of large interferometers, such as the VLTI and CHARA arrays with maximum baselines of

[★] The catalog is available in electronic form at the CDS via anonymous ftp to cdsarc.u-strasbg.fr (130.79.128.5) or via <http://cdsweb.u-strasbg.fr/cgi-bin/qcat?J/A+A/>

^{★★} Michelson Postdoctoral Fellow, formerly at LESIA, Observatoire de Paris.

202 and 330 m, respectively, motivated us to compile a catalog for longer baselines, hereafter Cat. 2.

In Sect. 2 we explain why the sensitivity of current interferometers leads us to take as calibrators partly resolved stars instead of point-like sources, in the bright star regime. Then, we argue that these stars can be safely modeled as uniform disks provided they are carefully selected, and we review two different strategies to make this selection. Last, we explain how to decide if a calibrator is appropriate for a given observation. In Sect. 4 we describe how we built Cat. 2 by using C99's method and infrared photometric measurements for stars fainter than those in Cat. 1. Finally, in Sect. 5 we discuss the main characteristics of Cat. 2. In particular we demonstrate the relevance of this new catalog for the VLTI/VISA (the VLT interferometer sub-array, involving the 1.8 m auxiliary telescopes) and the CHARA array.

2. Choosing and modeling calibrators

The ideal calibrator is a source for which the intrinsic visibility, using the same observational setup as the science target, can be perfectly predicted. Thus every calibrator needs to be described by a morphological model, so that its true squared visibility can be predicted for the full range of spatial frequencies that can be addressed by the interferometer. As reference sources are chosen among stellar objects, the most common models employed to describe a calibrator are, in increasing number of free parameters:

1. The point source (no free parameters): in that case $V_{\text{cal.}}^2 = 1$ at any baseline;
2. The uniform disk (UD model), with the angular UD diameter θ as the only free parameter: the monochromatic squared visibility is then given by the relationship:

$$V_{\text{UD}}^2(x) = 4 \left(\frac{J_1(x\theta)}{x\theta} \right)^2, \quad (3)$$

where J_n denotes the n th Bessel function of the first kind and x the spatial frequency, namely $\pi B/\lambda$ (B , baseline and λ the observing wavelength);

3. The limb-darkened disk (LD model), with two or more free parameters.

For simplicity and reliability, more complex calibrator models should be avoided. These include non-centrosymmetric or variable morphologies like pulsating or flare stars, fast rotators, and binary stars. Indeed, a good calibrator needs to be:

1. *Well modeled*, in the sense that the model which is used to describe the morphology of the object is as simple as possible, yet appropriate within the level of accuracy required for the visibility;
2. *Well known*: the free parameter(s) in the model need to be known with sufficient accuracy;
3. *Stable*: no time dependency of the morphology;
4. *Observable with the same setup* and in the same conditions as the science target, e.g. close to the target on the sky, with comparable magnitude and preferably spectral type.

It should be noted that these requirements are conflicting since in general they call for references much smaller than the science targets, yet having approximately the same color and apparent brightness, which is impossible for thermal sources. Therefore the choice of a calibrator will always be the result of a compromise. The first and last requirements exclude the point source model in almost every circumstance for long baselines, as it would imply an unrealistically small (hence faint) reference. For example, in order to induce a bias smaller than 1 % ($V^2 > 99\%$), a reference star considered as a point source with a 300 m baseline at $\lambda = 2.2 \mu\text{m}$ needs to have an angular diameter smaller than 0.1 mas. If the source is a K0 giant, this corresponds to an infrared magnitude $K \gtrsim 8$, beyond the sensitivity limit of interferometers with small or medium size telescopes (less than 2 m in diameter) without fringe tracking devices. For interferometers using larger telescopes, with a sensitivity limit close to or better than $K = 10$, it appears possible to find real non-resolved sources ($V^2 > 99\%$), because sensitivity is no longer an issue. Still, one has to be careful for the following reasons. A $K = 10$ star earlier than M5 will definitely be unresolved for a 200-m baseline interferometer operating in the near infrared, but one has to ensure that this particular candidate follows the chosen model, i.e. a point source. Following our previous discussion, the *well known* item is of no concern for an unresolved star, in the sense that no parameter drives the model, but the *well modeled* one still applies. For example, the candidate may be binary, just like the majority of main sequence stars (e.g. see Quist & Lindegren 2000). Therefore, non-sensitivity-limited interferometers still need well-modeled (thus *trustworthy*) calibrators. Considering that faint candidates ($K \gtrsim 8$) will arise from infrared photometric surveys, such as DENIS or 2MASS, for which very few supplementary data are available, the potential binarity will be very difficult to detect. It appears that there are two different cases for modern hectometric baseline stellar interferometers: the bright star regime ($K \lesssim 8$) and the faint star regime ($K \gtrsim 8$). Because one wants the interferometer to operate in the same regime for both the scientific target and the calibrator (e.g. with comparable signal to noise ratio), we advocate that an extension to the Bordé et al. (2002) catalog, containing only well-modeled (uniform disk ensured) and well known (high accuracy estimation of the angular diameter) objects will not only be useful for medium aperture arrays operating in the near infrared, such as the CHARA Array or the Palomar Testbed Interferometer (Colavita et al. 1999), but also for the VLTI/VISA interferometer using AMBER in the bright star regime.

It happens that quiet single stars can easily and correctly be modeled as uniform disks when the squared visibility exceeds $\approx 40\%$, as the difference between a UD and an LD model is then smaller than 0.1 % (see Fig. 1). Stellar angular diameters can be known from direct high-angular resolution measurements (interferometry or Lunar occultations) or estimated indirectly by (spectro-)photometry. We argue that a spectrophotometric estimate of the diameter is more suitable for reference purposes, because direct diameter measurements have only been performed on a limited number of sources (listed in the Catalog of High Angular Resolution Measurements (Richichi et al. 2004), hereafter CHARM), and most of these

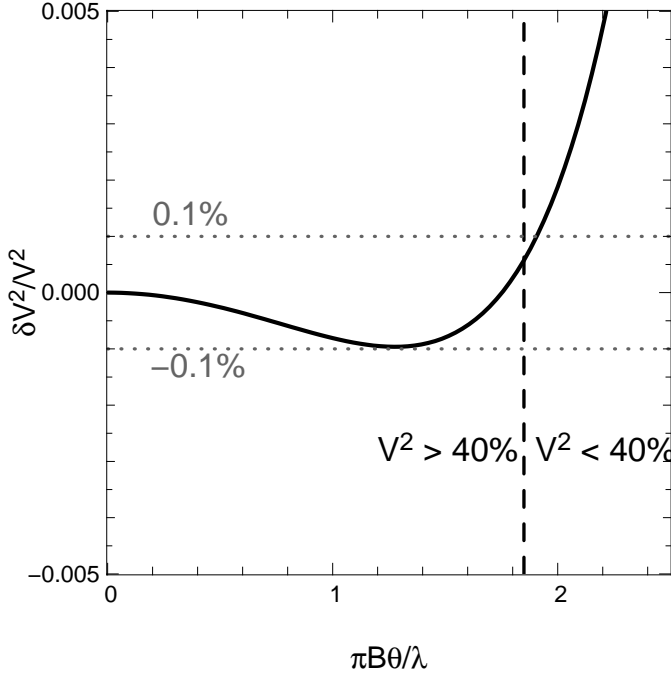


Fig. 1. Relative difference between UD and LD squared visibilities ($\delta V^2/V^2$) with respect to spatial frequency times angular diameter. The UD diameter is adjusted to minimize the quadratic deviation between UD and LD squared visibilities in the $V^2 > 40\%$ domain. This particular LD model represents the most limb-darkened disks of our catalog, namely for M0III stars in the J band. In the domain corresponding to $V^2 > 40\%$, the relative difference remains below 0.1 %. It is even smaller for less limb-darkened stars.

sources do not have the properties required for being a good calibrator at long baselines. Besides, this interferometric data set is in essence heterogeneous and, more specifically, UD values are published usually at a single wavelength. Because of limb darkening, these values are not readily valid for other band-passes. Therefore, in the absence of an exhaustive and homogeneous set of direct diameter measurements of suitable calibrator stars (a certainly much needed, however intensive, observational program), we prefer in the remainder of this paper to apply an indirect method to determine the diameters for a set of stars that are selected such that they can be trusted as single and stable.

At this point, two strategies have been proposed:

1. *A dynamic or open list approach:* software that queries existing databases for calibrator candidates in a given field is designed and distributed. The software is expected to help the observer in the down-selection process by using the information available in the databases. Then, it should provide either a direct estimate of the visibility at the time of the observation, or the parameter value(s) for a given visibility model (e.g. the UD angular diameter). Two examples of this approach are *Search Calibrator* integrated in the software ASPRO¹ issued by the Jean-Marie Mariotti

Center (Bonneau et al. (2004)), and *getCal*² issued by the Michelson Science Center;

2. *A static or closed list approach:* a catalog of carefully selected potential calibrators that includes all the necessary information to compute the visibility for any relevant baseline and bandpass is compiled and distributed. Such a list, the *ESO Calvin Tool*³, has been made available for the VLTI Mid-Infrared interferometer (MIDI, see Leinert et al. 2004).

We prefer the closed list approach for three reasons:

1. It enables a dedicated check on all of its entries, which would not be possible with a generic selection process;
2. The catalog can be revised and updated as some of its entries are found – either serendipitously or by means of a systematic interferometric survey – to be unreliable as a reference (the most likely reason being that they are hitherto unknown binaries), with the objective that eventually all bad entries will be removed;
3. Selecting a calibrator is easier for the beginner in interferometry since it can be hand-picked from a source list.

However, the dynamic approach has its merits as it could provide either specific calibrators missing in our catalog (e.g. stars earlier than K0), or standard calibrators for the faint star regime ($K \gtrsim 8$) where a closed list is unmanageable.

3. The calibrator decision diagram

The purpose of the calibrator decision diagram described here is to find the right calibrator for a given observation. In order to achieve the desired precision for a given instrumental configuration, calibrators also have to be selected according to their diameters and diameter errors. For the UD model, the stellar angular diameter contains all the knowledge of the source, thus the squared visibility error associated with the calibrator error is

$$\left(\frac{\sigma_{V_{\text{cal}}^2}}{V_{\text{cal}}^2} \right)_\theta = \left(\frac{\partial V_{\text{cal}}^2}{\partial \theta} \sigma_\theta \right) \frac{1}{V_{\text{cal}}^2} = 2x\theta \frac{J_2(x\theta)}{J_1(x\theta)} \frac{\sigma_\theta}{\theta}. \quad (4)$$

As the knowledge of the calibrator should not be the limiting factor on the precision of the visibility measurement, we require for the calibrator choice that the relative error in the squared visibility, $\sigma_{V_{\text{cal}}^2}/V_{\text{cal}}^2$, due to the uncertainty on the calibrator diameter alone, σ_θ/θ , should not exceed the internal (instrumental) error, σ_{μ^2}/μ^2 , that is to say

$$\left(\frac{\sigma_{V_{\text{cal}}^2}}{V_{\text{cal}}^2} \right)_\theta \leq \left(\frac{\sigma_{\mu^2}}{\mu^2} \right)_{\text{limit}}. \quad (5)$$

For further discussions, we set the upper limit on inequality (5) to 2 % as it implies for the relative error in the visibility an upper limit of $\sigma_V/V = 1\%$, the standard precision benchmark for single-mode interferometers in the literature. Examples of scientific results achieved with such a precision include the study of the internal structure of Sirius by

¹ <http://mariotti.ujf-grenoble.fr/~aspro/>

² <http://msc.caltech.edu/software/getCal/>

³ <http://www.eso.org/observing/etc/preview.html>

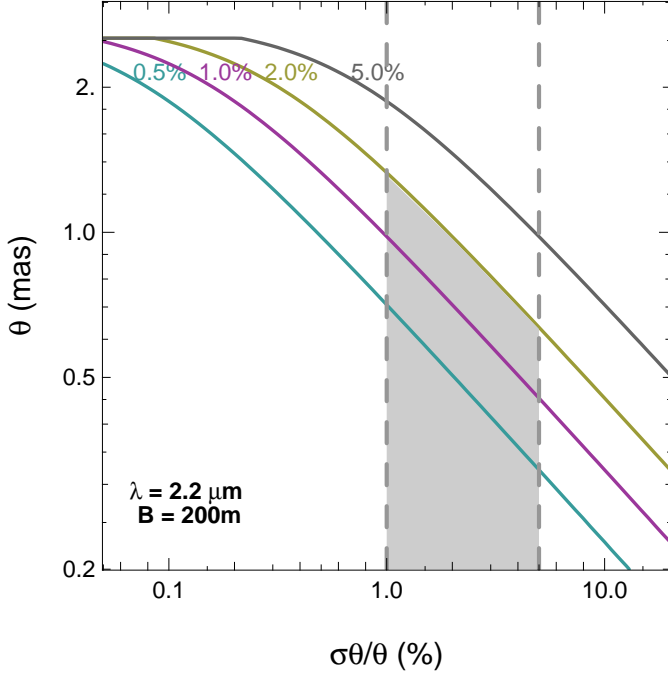


Fig. 2. Calibrator decision diagram (logarithmic scales) fixing the wavelength to $2.2 \mu\text{m}$ and the baseline to 200 m: contours of the instrumental precision as a function of the diameter and diameter error of the calibrator. Stars below a given contour could be used at the labeled precision. Vertical dashed lines delimit the area corresponding to the typical diameter error obtained through (spectro-)photometric determinations (1–5 %).

Kervella et al. (2003) or the test of the model atmosphere of a M4 giant by Wittkowski et al. (2004).

Inequality (5) can be turned into a *decision diagram* that helps decide whether a calibrator is suitable for a given observation. In the framework of the UD model, and leaving aside magnitude and spectral type considerations, a given source can be represented as a point in a diameter/diameter error plane, ie $(\theta, \sigma_\theta/\theta)$. We refer to this plane as the *calibrator plane*. As for the instrumental configuration, all needed information is embedded in the pair spatial frequency/instrumental precision, i.e. $(x, (\sigma_\mu^2/\mu^2)_{\text{limit}})$ or alternatively in the triplet wavelength/projected baseline/instrumental precision, ie $(\lambda, B, (\sigma_\mu^2/\mu^2)_{\text{limit}})$. By holding two of these three quantities fixed, one can plot the third as a function of the diameter and diameter error. We call this plot the *calibrator decision diagram*.

As a first example, we set in Fig. 2 the wavelength to $2.2 \mu\text{m}$, the baseline to 200 m, and we plot contours of the instrumental precision in the calibrator plane. In that case, if one wants $\sigma_{V_{\text{cal}}}^2/V_{\text{cal}}^2$ to be at most 2 %, the diagram shows that either $\theta \leq 1.3 \text{ mas}$ with a 1 % error or $\theta \leq 0.65 \text{ mas}$ with a 5 % error is required. It is noteworthy that for $\sigma_{V_{\text{cal}}}^2/V_{\text{cal}}^2 \leq 2 \%$ and $\sigma_\theta/\theta \geq 1 \%$, the squared visibility stays above 40 % (corresponding to a $\theta = 1.3 \text{ mas}$ star, observed at $\lambda = 2.2 \mu\text{m}$, with a 200 m baseline), which assures the validity of the UD model as discussed previously. For this reason we keep in the following

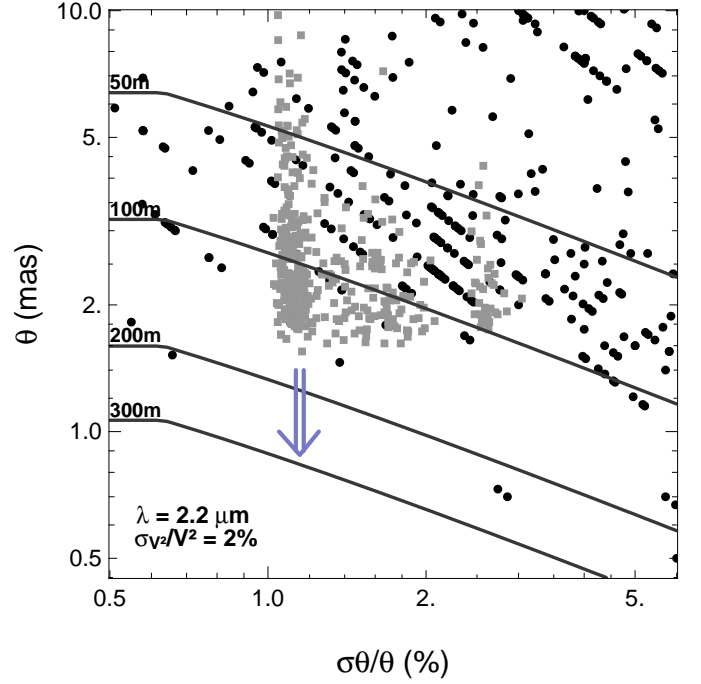


Fig. 3. Calibrator decision diagram (logarithmic scales) fixing the wavelength to $2.2 \mu\text{m}$ and the instrumental precision to 2 %: contours of the baseline as a function of the diameter and diameter error of the calibrator. Stars below a given contour can be used at the labeled baseline. Stars from Cat. 1 appear as gray squares and stars from CHARM as black dots. The double arrow indicates the direction we chose to follow to expand Cat. 1. The 50, 100, 200 and 300 m curves in the K band ($\lambda = 2.2 \mu\text{m}$) correspond respectively to 35, 75, 145 and 220 m in the H band ($\lambda = 1.6 \mu\text{m}$) and 25, 55, 110 and 165 m in the J band ($\lambda = 1.2 \mu\text{m}$).

these requirements on the squared visibility and angular diameter precisions.

As a second example, we set in Fig. 3 the wavelength to $2.2 \mu\text{m}$, the instrumental precision to 2 %, and we plot contours of the baseline in the calibrator plane. Black dots represent stars flagged as single and with no shell in CHARM, and gray squares represent stars from Cat. 1. Stars located below a given contour can be used as calibrators at the corresponding baseline. It appears from this plot that CHARM provides calibrators for projected baselines up to $\sim 70 \text{ m}$, and Cat. 1 for baselines up to $\sim 100 \text{ m}$, if one is not too stringent on the sky coverage.

4. Building the catalog

4.1. How to expand Cat. 1: better models or smaller stars?

Looking at Fig. 3, there are two ways in which Cat. 1 could be expanded to satisfy the 2 % precision at 200 m baselines:

1. Decrease the diameter errors by improving the calibrator models (going leftwards in the diagram);
2. Decrease the stellar diameters by finding smaller stars (going downwards in the diagram).

The first solution necessitates working with more resolved stars which requires more elaborate models than the UD, along with high-quality observations to determine the parameters of these models. Keeping with our objectives of simplicity and reliability, we favor the second approach, which consists in going only to smaller stars since we guarantee hereby the validity of the UD model. On the other hand, we have to be very careful not to degrade the error. The second solution features the drawback of working with fainter stars. Indeed, the angular diameter logarithmic scale in Fig. 3 can be viewed as a linear magnitude scale for a given spectral type (a given temperature).

4.2. Pushing the spectro-photometric method further

Through their whole series of papers Cohen et al. built an all-sky network of absolute reference sources for spectro-photometry in the infrared. The tenth paper, C99, exposes at length their method: by fitting low-resolution composite spectra to infrared photometric measurements, they derive both absolute spectral irradiances and stellar angular diameters. Their grid stars were selected from the IRAS Point Source Catalog (hereafter IRAS PSC) applying stringent quality criteria that qualify most of these stars as interferometric calibrators as well. Cat. 1 was then built by removing the very few stars that would depart from a UD at low resolution.

In their original work, C99 used the following 6 criteria for selecting calibrator candidates in the IRAS PSC:

1. The IRAS flux at $25\ \mu\text{m}$ must be greater than 1 Jy;
2. IRAS infrared colors are restricted to one particular quadrant, corresponding to giant stars;
3. IRAS candidates must be as normal as possible: sources flagged as non-stellar, variable, emission line or carbon stars are rejected;
4. Total IRAS fluxes within a radius of $6'$ must be less than 5 % of the infrared flux of the candidate;
5. IRAS stars must not be associated with a small extended source. The contribution of infrared cirrus must be less than 5% of the candidates infrared flux;
6. To reduce the chance of selecting variables, candidates must fall in one of the following spectral and luminosity classes:
 - A0–G9 and II–IV,
 - K0–M0 and III–V.

Stepping in the tracks of C99, we applied the previous set of criteria to the IRAS PSC, modifying criterion 1 to $F_{25\ \mu\text{m}} \leq 1\ \text{Jy}$ in order to sort out new stars. We also required the stars to be identified in the SIMBAD database to make possible further quality filtering (criteria 3 and 6). A total of 8313 stars passed criteria 1 and 2, as well as the identification in SIMBAD. In the selection process we found that the 5th criterion – meant to remove stars blended with interstellar cirrus – severely impairs the sky coverage around the Galactic Equator. Therefore, we decided to leave that criterion aside, and to rely instead on the quality of the spectrum fit to the infrared photometric measurements.

4.3. Discarding candidates that depart from a UD

Multiplicity and variability are the main causes of departure from a UD that one would like to avoid. Ideally, multiple stars should be rejected according to the separation and contrast between the components. As thresholds for these quantities could only be determined according to the instrument configuration and characteristics (baseline, wavelength, accuracy, etc.), we chose to remove all known spectroscopic and astrometric binaries on the basis of their SIMBAD object type. However, because of SIMBAD's hierarchical classification, a star can have a companion without being classified as a binary. For this reason, we also used the Catalog of Visual and Double Stars in Hipparcos (Dommanget & Nys 2000) to remove all stars with a companion within $2'$. This distance represents a safe upper limit for any pointing devices or tip-tilt servos. In addition, the Hipparcos Catalog (Perryman et al. 1997) was used in order to remove known variables, as well as stars with a positive “Proxy” flag, ie having field stars within $10''$. The $2'$ and $10''$ thresholds make the catalog useful for a wide variety of instruments without affecting significantly the number of stars left in the catalog (only 12 % of the stars were discarded).

In order to pin down more variable stars or unresolved binaries, we used several radial velocity catalogs, starting with the catalog by Malaroda et al. (2001) who collected all radial velocity measurements from the literature until 1998. Every entry of this catalog contains the nature of the object according to every author. If a single author suspected a star to be a spectroscopic binary, we discarded that candidate. Furthermore, we looked at de Medeiros & Mayor (1999) and Nidever et al. (2002) for post-1998 measurements and used them in same manner as Malaroda et al. (2001). This process led us to remove an additional 1 % of our candidates.

A last cause of departure from the symmetric UD model would be oblateness due to fast rotation. This should not be a concern in our stellar sample as it contains only G8–M0 giants expected to be slow rotators. We checked that by using $v \sin(i)$ as a proxy for the rotation rate: indeed, for all 36 stars with measurements, we found that $v \sin(i) < 10\ \text{km/s}$.

As a general remark, let us point out that, considering the large number of candidate stars, it was out of the question to check every one of them in the literature, and to perform dedicated observations where it would have appeared necessary. Therefore, we would like to draw the attention of the reader to the fact that a few stars which are not suitable for calibration may remain in our published list.

4.4. Photometry

Deriving angular diameters with C99's method requires absolute photometric data between 1.2 and $35\ \mu\text{m}$. We used $12\ \mu\text{m}$ and $25\ \mu\text{m}$ photometric data from the IRAS PSC (our input catalog), as well as those from the IRAS FSC (Faint Source Catalog). We extracted the near-infrared photometry, H and Ks magnitudes, from the Two Micron All Sky Survey Point Source Catalog (hereafter 2MASS PSC) with the absolute calibration by Cohen et al. (2003). The 2MASS PSC was the only near-infrared catalog that matches our needs in terms of sky cover-

age. However, we had to deal with a poor photometric precision ($\sigma_K = 0.25$) for the bright stars ($K = 3-4$) we are interested in, as they tended to saturate the 2MASS detectors. Finally, the MSX infrared Astrometric Catalog (Egan & Price 1996) provided 6 photometric data points in the $4.22 - 4.36 \mu\text{m}$ (B1 band), $4.24 - 4.45 \mu\text{m}$ (B2 band), $6.0 - 10.9 \mu\text{m}$ (A band), $11.1 - 13.2 \mu\text{m}$ (C band), $13.5 - 16.9 \mu\text{m}$ (D band) and $18.1 - 26.0 \mu\text{m}$ (E band) infrared bands. These last measurements were converted into absolute photometric measurements using the Cohen et al. (2000) calibration.

We looked for interstellar extinction by computing the spectral class photometry (especially B-V), and comparing it to its expected value. If A_λ is the extinction in magnitude, the interstellar medium is characterized by $R_V = A_V/(A_B - A_V) = A_V/E_{B-V}$. We used an average of $R_V = 3.1$. Then, thanks to the tables of A_λ/A_V from Cardelli et al. (1989), we corrected the H and K magnitudes for reddening. However, this correction always stays within the photometric error bars, because our candidates are bright stars that are close and for which 2MASS photometry is not very accurate. Therefore our relatively crude estimation of the reddening is appropriate.

4.5. Deriving limb-darkened diameters from stellar templates

Stellar templates computed by C99 consist of absolute composite spectra for different spectral types and luminosity classes, together with limb-darkened (LD) angular diameters ϕ . Because C99 used plane-parallel Kurucz model atmospheres, their LD angular diameters (ϕ) correspond to Rosseland angular diameters, associated with a Rosseland optical depth of unity. Indeed, this diameter corresponds to the zone where photons from the continuum are emitted, and where the limb brightness drops to zero. For plane-parallel models the Rosseland diameter is equal to the limb darkened diameter ϕ (see discussion in Wittkowski et al. (2004)).

After retrieving the spectral types and luminosity classes of our candidate calibrators from SIMBAD, we fitted the absolute template corresponding to a specific star to its infrared photometric measurements. All photometric measurements were converted into isophotal quantities, following the calibration prescribed by C99 for IRAS PSC and FSC, by Cohen et al. (2003) for 2MASS PSC and Cohen et al. (2000) for MSX. Fig. 4 shows two examples of stellar template fits.

The scaling factor resulting from the fit, l , yielded the LD diameter of the star

$$\phi = \sqrt{l} \times \phi_{\text{ref}}. \quad (6)$$

For every diameter, we computed an associated error by taking into account the contributions of the fitting formal error, σ_l , corresponding to $|\chi^2(l) - \chi^2(l \pm \sigma_l)| = 1$, and of the original template diameter error, $\sigma_{\phi_{\text{ref}}}$, according to

$$\left(\frac{\sigma_\phi}{\phi}\right)^2 = \left(\frac{\sigma_l}{l}\right)^2 + \left(\frac{\sigma_{\phi_{\text{ref}}}}{\phi_{\text{ref}}}\right)^2. \quad (7)$$

We could not find in C99 the angular diameter errors of their original templates. By comparing the diameters published

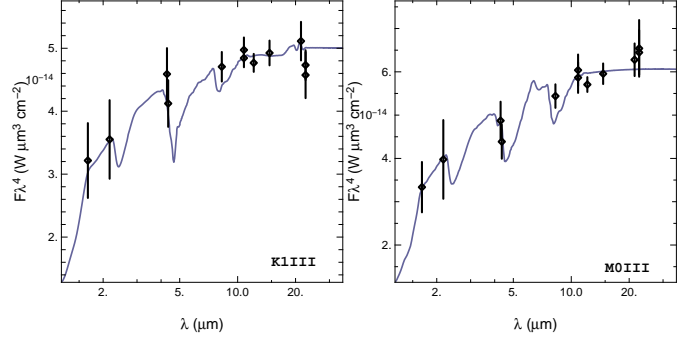


Fig. 4. Examples of stellar template fits to photometric measurements converted into monochromatic irradiances at isophotal wavelengths. The data points stand for (from left to right): H, K_s (2MASS), B1, B2, A (MSX), $F_{12 \mu\text{m}}$ (IRAS PSC and FSC), C, D, (MSX) and $F_{25 \mu\text{m}}$ (IRAS PSC and FSC). *Left:* HD 15248, a K1III star ($\chi_r^2 = 0.66$). *Right:* HD 164724, a M0III star ($\chi_r^2 = 0.83$).

by these authors and the ones computed by our implementation of their method, this internal error was determined to be $\sigma_{\phi_{\text{ref}}}/\phi_{\text{ref}} = 1.03\%$. This value appeared to be independent of spectral type and luminosity class.

As mentioned at the end of Sect. 4.2, we used the quality of the template fit as a filtering tool to ensure the consistency of our method. Namely, if the reduced χ^2 , i.e. $\chi_r^2 = \chi^2/(N - P + 1)$, where N is the number of data points and P the number of parameters, is greater than 1, we exclude the star from the final selection.

4.6. From limb-darkened to uniform disk diameters

We converted LD diameters into UD diameters in the J, H and K bands by using the following four-coefficient limb-darkening law from Claret (2000)

$$I(\mu) = 1 - \sum_{k=1}^4 a_k (1 - \mu^{k/2}), \quad (8)$$

where I is the specific intensity and μ the cosine of the angle between the line of sight and the perpendicular to the stellar surface. Claret (2000) has tabulated the coefficients a_k according to the stellar effective temperature T_{eff} and surface gravity $\log(g)$.

Only 65 of our candidates could be found in the Cayrel de Strobel et al. (2001) catalog of effective temperature and surface gravity measurements, all of them with a spectral type G8–K4. For all others, we estimated T_{eff} by using the Bessell et al. (1998) polynomial relation based on the color index $V - K$. When no measurements were available, we used the typical surface gravity for the spectral class, as well as solar abundances. This is legitimate since the infrared limb-darkening is not very sensitive to these parameters.

Taking into account a center-to-limb variation, the visibility function becomes

$$V_{\text{LD}}(x) = \frac{\int_0^1 I(\mu) J_0(x \phi \sqrt{1 - \mu^2}) \mu d\mu}{\int_0^1 I(\mu) \mu d\mu}. \quad (9)$$

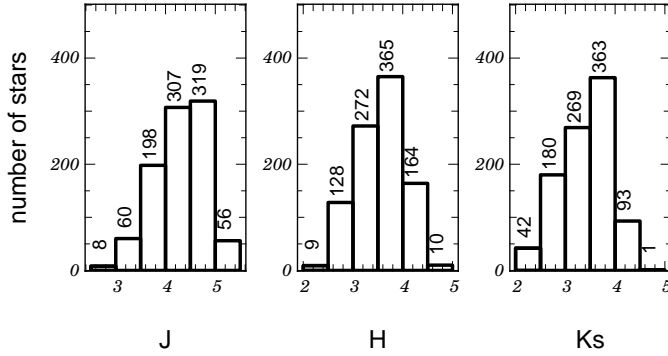


Fig. 5. Histograms of magnitudes

UD diameters in the J, H, and K were obtained by fitting V_{UD} (Eq. (3)) to V_{LD} (Eq. (9)) in the domain of validity of the UD model, i.e. $V^2 \geq 0.4$. In this domain, the relative difference between the two visibility profiles is less than 10^{-3} (see Fig. 1 for the most darkened disk of our sample, namely M0III stars in the J band).

5. Major characteristics of the catalog

5.1. Electronic version

An electronic version of the catalogue is available online from the Centre de Données astronomiques de Strasbourg (CDS). For every calibrator star, it provides:

1. Identifiers: HD and HIP numbers;
2. Coordinates: ICRS 2000.0 right ascension and declination, proper motion, and parallax;
3. Physical properties: spectral type;
4. Photometric measurements: B and V from SIMBAD, J, H, and Ks from 2MASS PSC, $12\mu\text{m}$ from IRAS;
5. Angular diameters: LD diameter and UD diameters for J, H and K. A single error is given for all of them, since the correction on this quantity due to the center to limb variation is very small;
6. Ancillary information: variability and multiplicity flags, variability type from Hipparcos. This category is meant to distinguish between stars for which no variability nor companion has been detected and stars for which no information is available.

5.2. Infrared magnitudes

On Fig. 5 we plotted three histograms for J, H, and Ks infrared magnitudes. The median magnitudes are 4.3 in J, 3.6 in H, and 3.5 in Ks.

5.3. Sky coverage

Cat. 2 overall sky coverage is such that there is always a calibrator closer than 10° whatever the location on the sky (Table 1). Moreover, if we keep only stars that can achieve a 2% visibility error for baselines greater than 200 m in K (145 m in H, 110 m in J), the calibration appears to be still feasible for more than half the sky. The northern hemisphere

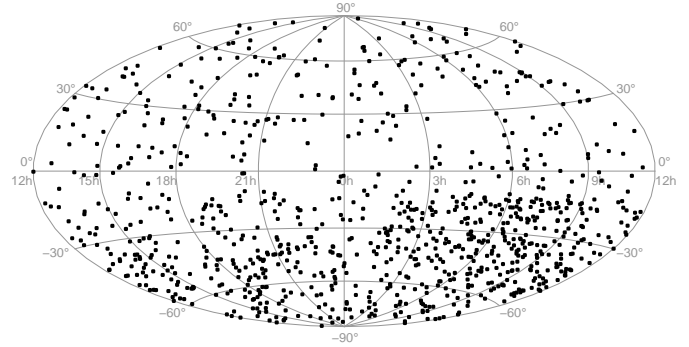


Fig. 6. Sky coverage of Cat. 2 in equatorial Hammer-Aitoff representation.

Dist. to the closest calib.	Northern Hem.	South. Hem.
less than 3.75°	45 % (15 %)	85 % (53 %)
less than 5°	75 % (45 %)	95 % (65 %)
less than 10°	99 % (85 %)	100 % (89 %)

Table 1. Sky coverage characteristics: area of the sky having corresponding distance to the closest calibrator. Details for northern (positive declination) and southern (negative declination) hemispheres are given. The number in brackets correspond to a reduced version of Cat. 2, containing only stars that can achieve a 2% visibility error for baselines greater than 200 m in K (which corresponds to 145 m in H, 110 m in J).

happens to be less populated than the southern one (Fig. 6), because more stars were filtered out in this part of the sky because of an unsatisfactory spectral type identification with SIMBAD. For the southern hemisphere, spectral identification comes from the Michigan Catalogue of Two-dimensional spectral types (Houk & Cowley 1975), which offers better spectral type identification than what is available from any studies in the northern hemisphere.

5.4. Baseline range

Fig. 7 shows a comparison between Cat. 1 and 2 in the *calibrator decision diagram* (observations in the K band with a 2% precision on the visibility), and illustrates the significant gain due to this work. Cat. 2 can be used to achieve a 2% visibility error on the whole sky with baselines up to ~ 100 m, ~ 130 m, and ~ 180 m, in the J, H and K bands, respectively (see Table 2 for details). Therefore, our extended calibrator catalog fulfills the needs for calibration of the VLTI, the CHARA array, and any other 200-m class interferometers in the near infrared.

6. Conclusion

We have presented a list of 1320 stars selected to serve as calibrator stars for long baseline stellar interferometry. Among them, 374 come from the previous catalog compiled by Bordé et al. (2002). The selection of the new stars was made according to the spectro-photometric criteria defined by C99, as well as additional ones that are specific to near-infrared interferometry. We used the work by C99 to estimate the angu-

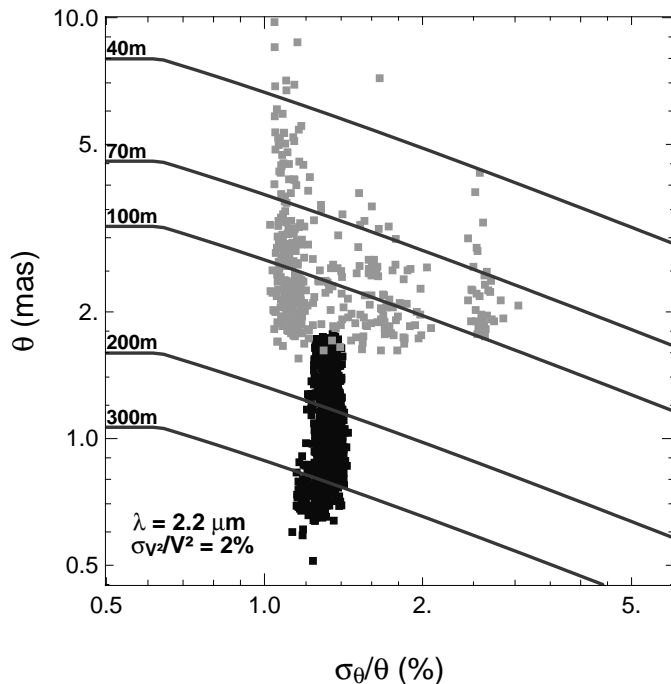


Fig. 7. Comparison of Cat. 1 (gray dots) and 2 (black dots) in the calibrator decision diagram. The 50, 100, 200 and 300 m curves plotted here, for the K band ($\lambda = 2.2 \mu\text{m}$), corresponds respectively to 35, 75, 145 and 220 m in the H band ($\lambda = 1.6 \mu\text{m}$) and 25, 55, 110 and 165 m in the J band ($\lambda = 1.2 \mu\text{m}$).

Band	$\sigma_{V^2}/V^2_{\text{cal.}}$		
	1 %	2 %	3 %
J	40 → 91 m	55 → 125 m	65 → 150 m
H	55 → 121 m	75 → 167 m	85 → 200 m
K	75 → 163 m	100 → 224 m	120 → 266 m

Table 2. Improvement of the median maximum baseline for the J, H, and K bands at the 1, 2, and 3 % visibility precision levels between Cat. 1 and 2.

lar diameter from infrared photometric measurements extracted from IRAS, 2MASS and MSX Astrometric catalogs. Our new catalog of interferometric calibrators is a homogeneous set of stars, provided with limb-darkened angular diameters and uniform disk angular diameters in the J, H and K bands. Its intrinsic characteristics – a small list of stars with accurate angular diameters and uniform sky coverage – inherited from the previous version, were carefully maintained, while we included smaller stars in order to fulfill the needs of 200-m class interferometers like the VLTI in the H band (and redder) in the bright star regime ($K \lesssim 8$), and the CHARA array in the K band (and redder). In this paper, we improved the usefulness of Cat. 2 with respect to Cat. 1 by extending the selection to fainter stars (this corresponds to going downwards in the calibrator decision diagram of Fig. 3). As all eligible stars from the IRAS survey have been used in Cat. 2, further extension is not possible in this direction. Improvements could still be obtained if/when more accurate photometry becomes available, which will result in smaller diameter errors (this corresponds to going

leftwards in the calibrator decision diagram). For this, a dedicated observing program is needed, as most of these sources are too bright for the major infrared surveys. From the decision diagram it can be seen that the gain to be expected is in a better sky coverage at 200–300 m baselines, rather than an extension of the maximum baseline for which Cat. 2 would be useful.

Acknowledgements. We would like to thank the referee for his valuable corrections, suggestions and comments. It is a pleasure to thank Stephen T. Ridgway and Jason P. Aufdenberg for valuable discussions, suggestions and corrections concerning the present work. This work has made use of the SIMBAD database, operated at CDS, Strasbourg, France. It also has made use of data products from the Two Micron All Sky Survey, which is a joint project of the University of Massachusetts and the Infrared Processing and Analysis Center/California Institute of Technology, funded by the National Aeronautics and Space Administration and the National Science Foundation. This work was performed in part under contract with the Jet Propulsion Laboratory (JPL) funded by NASA through the Michelson Fellowship Program. JPL is managed for NASA by the California Institute of Technology.

References

- Bessell, M. S., Castelli, F., Plez, B., 1998, *A&A*, 333, 231
 Bonneau, D., Clausse, J.-M., Delfosse, X., et al., to be published in the proceedings of conference “New frontiers in stellar interferometry” SPIE 5491, 2004
 Bordé et al., 2002, *A&A*, 393, 183
 Cayrel de Strobel, G., Soubiran, C., Ralite, N., 2001, *A&A*, 373, 159
 Cardelli, J. A., Clayton, G. C., Mathis, J. S., 1989, *ApJ*, 345, 245
 Claret, A., 2000, *A&A*, 363, 1081
 Cohen, M., Russel, G. W., Carter, B., et al., 1999, *AJ*, 117, 1864 (C99)
 Cohen, M., Hammersley, P., Egan, M., 2000, *AJ*, 120, 3362
 Cohen, M., Wheaton, Wm., A., and Megeath, S., T., 2003, *AJ*, 126, 1090
 Colavita, M. M., Wallace, J. K., Hines, B. E., et al., 1999, *ApJ*, 510, 505
 de Medeiros, J.R., Mayor, M., 1999, *A&AS*, 139, 433
 Dommange, J., Nys, O., 2000, *A&A*, 363, 991
 Egan, M., Price, S., 1997, *AJ*, 112, 2862
 Glindemann, A., Algomedo, J., Amestica, R., et al. 2003, in *Interferometry for optical astronomy II*, ed. Wesley A. Traub, Proc. SPIE, 4838, 89
 Houk, N., Cowley, A.P., Michigan Catalogue of two dimensional spectral types for the HD stars. Ann Harbor, Univ. of Michigan, 1975
 Kervella, P., Thévenin, F., Morel, P., Bordé, P., 2003, *A&A*, 408, 681
 Kervella, P., Ségransan, D., Coudé du Foresto, V., 2004, *A&A*, 425, 1161
 Leinert, C., Graser, U., Waters, L.B.F.M., et al., 2003, in *Interferometry for Optical Astronomy II*. ed. Wesley A. Traub, Proc. SPIE, 4838, 893
 Malaroda, S., Levato, H., Galliani, S., 2001, *Vizie Online Data Catalog III/216*
 Nidever, D. L., Marcy, G. W., Butler, R. P., Fischer, D. A., Vogt, S. S., 2002, *ApJS*, 141, 503
 Perrin, G., Coudé du Foresto, V., Ridgway, S.T., et al. 1998, *A&A*, 331, 619
 Perryman, M. A. C., Lindegren, L., Kovalevsky, J., et al., 1999, *A&A*, 323, 49
 Petrov, R., Malbet, F., Richichi, A., et al., 2002 in *Interferometry for Optical Astronomy*. ed. Pierre Léna and Andreas Quirrenbach, Proc SPIE, 4006, 68

- Quist, C.F., Lindegren, L., 2000, A&A, 361, 770
- Richichi, A., Percheron, I., Khristoforova, M., 2004, A&A, in press
- ten Brummelaar, T. A., McAlister, H. A., Ridgway, S. T., et al., 2003,
in Interferometry for Optical Astronomy II. ed. Wesley A. Traub,
Proc. SPIE, 4838, 69
- Wittkowski, M., Aufdenberg, J. P., Kervella, P., 2004, A&A413, 711